

Cover Page



Universiteit Leiden



The handle <http://hdl.handle.net/1887/22617> holds various files of this Leiden University dissertation.

Author: Celler, Katherine Anna

Title: A multidimensional study of streptomyces morphogenesis and development

Issue Date: 2013-11-27

CHAPTER 3

Single Particle Tracking of Dynamically Localizing TatA Complexes in *Streptomyces* Species

Katherine Celler, Gilles P. van Wezel, Joost Willemsse

ABSTRACT

The Tat (twin-arginine translocation) pathway transports folded proteins across the bacterial cytoplasmic membrane and is a major route of protein export in the mycelial soil-dwelling bacterium *Streptomyces*. We recently examined the localization of Tat components (TatABC) in time-lapse imaging and demonstrated that all three components colocalize dynamically with a preference for apical sites. Here we apply an in-house single particle tracking package to quantitatively analyze the movement of the TatA subunit, the most abundant of the Tat components. Segmentation and analysis of trajectories revealed that TatA transitions from free to confined movement and then to fixed localization. The sequence starts with a mixed punctate and dispersed localization of TatA oligomers, which then develop into a few larger still foci, and finally colocalize with TatBC to form a functional translocation system. It takes 15-30 min for the Tat export complex to assemble and most likely become active. With this study we provide the first example of quantitative analysis of dynamic protein localization in *Streptomyces*, which is applicable to the study of many other dynamically localizing proteins identified in these complex bacteria.

INTRODUCTION

In recent years, high resolution cell-biology techniques have revealed that, despite their small size, bacteria have a complex internal organization (Celler *et al.* 2013; Lopez and Kolter 2010; Margolin 2009). Molecular crowding within cells results in a dynamic equilibrium of components (Ellis 2001), leading to their non-uniform spatial distribution (Capoulade *et al.* 2011). This necessitates diffusion or active transport to areas where proteins can function, such as in nuclear organization, cell division or differentiation (McCormick and Flårdh 2012; Figge *et al.* 2004). *In vivo* multidimensional fluorescence microscopy allows scientists to visualize these processes which often display rapid and directed spatial relocation of proteins in three-dimensional time lapse movies (Mika and Poolman 2011; Meyer and Dworkin 2007; Shapiro *et al.* 2009). Taking cell division proteins as an example, these have been seen oscillating from one end of the cell to the other, forming rings across its midsection, or focal complexes at specific intracellular sites (Erickson *et al.* 2010; Hu and Lutkenhaus 1999; Noens *et al.* 2007; Raskin and de Boer 1999). To better understand these modes of action, and the lifespan of cellular proteins, quantitative measurements of protein abundance and dynamics are necessary.

A challenging subject for the study of dynamic protein localization is the Gram-positive filamentous soil bacterium *Streptomyces*. These mycelial organisms are used as natural producers of a large number of commercially important secondary metabolites, enzymes, and other secreted protein products (Hopwood 2007; Horinouchi 2007). In most bacteria the Sec pathway is the predominant route for protein export, but the streptomycetes encode an unusually large numbers of Tat (twin-arginine translocation) substrates (Palmer and Berks 2012; Müller and Klösgen 2005; Widdick *et al.* 2006). During fermentation, growth of hyphae is a balance of tip extension, branching frequency and fragmentation (Celler *et al.* 2012; Nieminen *et al.* 2013), all of which affect the efficiency of production and secretion. Fragmentation of hyphae strongly enhances protein secretion (van Wezel *et al.* 2006), which correlates well with our observation that the components of the Tat pathway in *Streptomyces* localize at the apical sites of hyphae (Willemse *et al.* 2012). A better understanding of where and when secretion takes place in the hyphae can lead to important insights for strain-improvement and rational process design.

The *Streptomyces* Tat machinery consists of TatA, TatB and TatC proteins (Widdick *et al.* 2006; Schaerlaekens *et al.* 2001), functional homologs of proteins found in Gram-negative bacteria such as *Escherichia coli* (Hicks *et al.* 2006). The tetrameric TatA is the most abundant component of the Tat complex (Jack *et al.* 2001) and many copies of this monotopic

membrane protein are believed to cluster around a substrate-bound TatBC complex to bring about the transport of a folded protein across the membrane, with an average of ~25 TatA subunits per complex (Dabney-Smith *et al.* 2006; Leake *et al.* 2008; Mori and Cline 2002).

Analysis of the Tat complex using live imaging revealed that the proteins localize surprisingly dynamically throughout the life cycle (Willemse *et al.* 2012). The dynamic localization of the separate components, however, creates difficulty in understanding their biological implication. Quantitative description and modeling of these movements by single particle tracking is therefore necessary to better understand complex assembly in time and space. Here we provide a detailed analysis of the dynamics of the TatA component of the Tat protein export pathway, using an in-house foci tracking package which was developed in the frame of the Particle Tracking Challenge of the International Symposium on Biomedical Imaging (ISBI) in 2012 (Chenouard *et al.*, *submitted for publication*). Specific questions we wished to address were (1) whether TatA undergoes different stages of motion prior to colocalization with TatB and TatC; (2) if so, what are the durations of these transitional stages; and (3) what is the time it takes for the complex to assemble.

This is the first mathematical tracking analysis of diffusion-limited foci in vegetative and aerial hyphae of *Streptomyces*, which can be applied to study the movement of many other dynamic proteins in these complex microorganisms.

MATERIALS AND METHODS

Strains and culturing conditions

Strain BRO3 is a derivative of *Streptomyces coelicolor* FM145, a variant of *S. coelicolor* M145 with reduced autofluorescence (Willemse and van Wezel 2009). BRO3 produces TatA-eGFP from the native chromosomal location (FM145, *tatA::tatA-eGFP*). Construction of the strain is described elsewhere (Willemse *et al.* 2012). To culture samples for live imaging, uncoated μ -dishes (Ibidi GmbH) were perforated at the side while closed tightly, and subsequently were semi-filled with SFM medium (Kieser *et al.* 2000). These dishes were inoculated with 1 μ L of spores at a concentration of 10⁹ spores/mL, turning the lid so that it was supported on the vents, allowing for gas exchange, and were sealed off by two layers of Parafilm to prevent drying of the medium. Samples were incubated at 30 °C for 48 hours before being transferred to the live imaging microscope. Temperature was controlled with a p-insert heating block and kept at 30 °C, and allowed to calibrate for one hour before commencing imaging.

Data collection

Fluorescence microscopy

Fluorescence and corresponding light micrographs were obtained with a Zeiss Observer inverted fluorescence microscope (with an Hamamatsu CCD camera at a resolution of 78 nm/pixel) as described (Willemse and van Wezel 2009; Jyothikumar *et al.* 2008). The green fluorescent images were created using 470/40-nm bandpass excitation and 525/50 bandpass detection. All images were background-corrected setting the signal outside the hyphae to 0 to obtain a sufficiently dark background. These corrections were made using Axiovision software 4.8.

Time-lapsed (live) imaging

Imaging was performed with a Zeiss Observer A1 microscope with a Hamamatsu EM-CCD C9100-02 camera as described (Willemse *et al.* 2011). Images were taken at 2 minute intervals with an exposure time of 100 ms. In order to minimize focal drift, the microscope stage and imaging chamber were allowed to equilibrate for 60 min before imaging. Initially z-stacks of 5 images with a focal depth of 0.5 μm were taken to prevent out-of-focus movement of the hyphae. These image sequences were then z-projected using the average z-stack projection method implemented in ImageJ.

Computer programs

The particle tracking algorithm was submitted to the Particle Tracking Challenge (<http://bioimageanalysis.org/track/>) of the 2012 International Symposium on Biomedical Imaging (<http://www.biomedicalimaging.org/2012/>), in which the performance of existing and newly developed particle tracking algorithms was tested against synthetic image sets with ground truth data. The methods and results of the challenge have been described (Chenouard *et al.*, *submitted for publication*). For details on the algorithm see the Supplemental Methods. The algorithm was implemented in the Java programming language (Sun Microsystems Inc., Santa Clara, CA) in the form of a plug-in for ImageJ (National Institutes of Health, Bethesda, MD), the computer-platform independent public domain image analysis program inspired by NIH-Image. ImageJ version 1.46o was used with the Java 1.7 compiler.

RESULTS AND DISCUSSION

We focused on TatA complex assembly as a whole, which occurs at a timescale several orders of magnitude greater than the fast movement of individual proteins. To capture an entire localization sequence (with an initial estimated duration of roughly 30-60 minutes) prior to bleaching of the samples, we took images for up to 3.5 hours at 2 minute intervals. Since mobility data suggests that cytosolic diffusion occurs at a time scale two orders of magnitude faster than membrane diffusion, we observed the dynamics of slow-moving membranebound macrocomplexes, and not the cytosolic fraction of TatA. *Streptomyces coelicolor* FM145, a derivative from the wild-type strain with reduced autofluorescence (Willemse and van Wezel 2009), was used for the localization studies, allowing imaging of the fluorescently labeled proteins at significantly higher signal to noise ratio. In 18 time lapse imaging movies of diffusion-limited TatA-eGFP, roughly 1500 foci were tracked from the onset of imaging to final localization. Foci tracked/detected in only two consecutive frames were not taken into account. The distribution of tracks (Figure 1) demonstrates that short tracks predominate, with roughly half of all tracks corresponding to 10 or less consecutive frames.

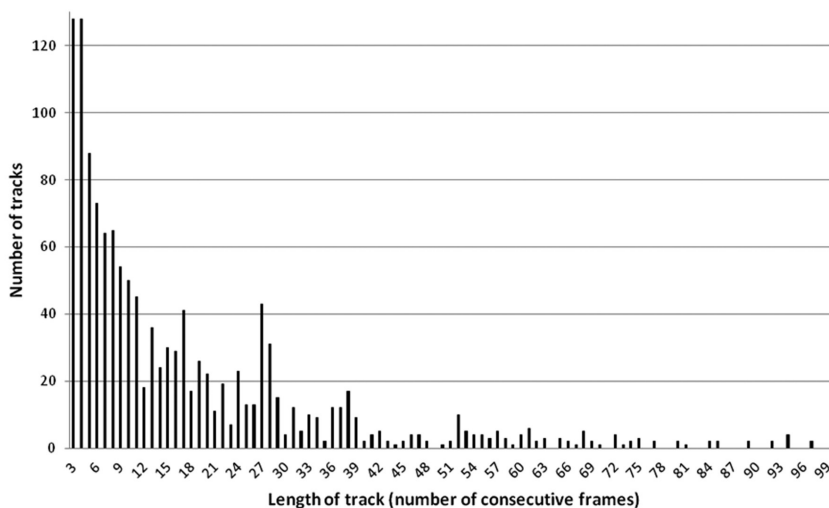


Figure 1. The distribution of tracks per track length demonstrates that short tracks predominate, with roughly 25% of TatA-eGFP foci tracked in three, four or five consecutive frames. These short tracks are of the many small TatA oligomers which race through the hyphae before agglomerating and forming larger complexes. Foci tracked in only two frames were not taken into account by the software. Roughly 50% of tracks are 10 consecutive frames or shorter.

Our previous study revealed increased amounts of localization in aerial hyphae, and imaging was therefore performed on early aerial hyphae after 48 hours of growth. At this point, many hyphae had already stopped growing due to crowding in the sample, but occasionally extending tips were still observed. In the growing hyphae, the Tat complex was seen following the tips. The broad range of stoichiometries exhibited by TatA suggests that dynamic polymerization and depolymerization occurs during assembly (Leake *et al.* 2008). This is evident in our time lapse sequences, where protein complexes display different types or stages of movement prior to fixed localization (ex. Fig. 2 and Supplemental Video 1). At the start of imaging, mainly dispersed fluorescence is seen, with gradually many faint foci appearing to ‘race’ along the hyphae. During this fast movement, several strong fluorescent foci become visible localizing (mainly) near the tips at roughly a 2 μm distance. Over the course of the time lapse, the faint foci either fade or merge with larger stable fluorescent foci. These faint foci have short tracks lasting only 3-4 frames or 6-8 minutes. Particle tracking highlights these tracks as brief directed bursts of motion. The larger foci remain stationary, or wobble before stabilizing.

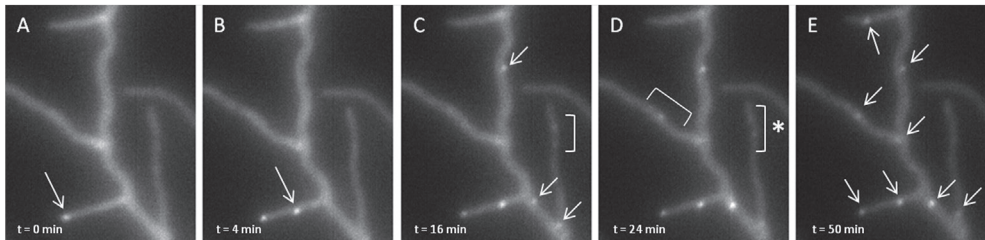


Figure 2. TatA-eGFP localizes dynamically in a *Streptomyces* hypha showing different stages of movement (frames taken from Supplemental Video 1). The initial localization is diffuse (A), though one focal point of TatA-eGFP localised to a branch tip can already be seen at this point in time (arrow). A second focus appears during live imaging (B), and around 15 minutes after the start multiple small foci are observed (C), some of which are clearly evident in the still frame (arrows), and some appearing as faint traveling foci in the time lapse (bracket). Foci continue to travel as they dynamically localise (D). Some foci ultimately fade again (bracket denoted by *) while others persist. In the final frame (E), multiple fixed localizations of the now stably localised protein are observed (arrows). Scale bar, 5 μm . Imaging was started at 49 hours post inoculation (48 hours of growth, with one hour of incubation time in the microscope). This time was deemed $t=0$.

A large variation in fluorescence intensity is seen over the course of imaging. Initial faint foci assemble over the course of the time lapse imaging to form complexes with increased fluorescent intensity, likely reflecting natural protein oligomerization.

Although formation of protein complexes can be enhanced by an eGFP fusion, which may affect protein functionality (Landgraf *et al.* 2012), we previously demonstrated that the TatA fusion is fully functional, restoring secretion of Tat substrates to wild-type levels. For full functional analysis of the TatA fusion product and Tat complex formation we refer to our previous work (Willemse *et al.* 2012).

Supplemental Video 2 shows another representative example of dynamic localization. The final image from the time lapse is presented (Fig. 3A), with the detected TatA-eGFP tracks projected onto the image. Despite the fading of foci due to the imaging, three tracks could be followed for the entire duration (one hour) of the movie. The trajectories of these tracks were plotted (Fig. 3B), demonstrating representative trajectories of a still focus, a rapidly traveling focus (which becomes confined after 10 minutes) and a wobbling focus.

Plotting of the mean square displacement (MSD, see Supplemental Data S1) versus time for these tracks (Fig. 3C) facilitated classification of the different modes of motion observed. In this case, MSD curves reflect the global changes that occur during complex assembly, and not rapid-scale protein dynamics. In the case of the wobbling focus, the MSD is irregular and does not show a clear trend towards a particular mode of diffusion. The trajectory of the traveling focus appears to consist of two different stages, namely an initial phase of rapid diffusion followed by a phase of slower diffusion. The still focus has an MSD curve with a slope of zero. Analysis was done for the first half of time lags for these curves, or 30 minutes, to minimize error.

Supplemental Video 3 shows a third example of the dynamic localization patterns described above (for still images see Fig. 4). The tracks of detected foci projected onto the image (Fig. 4A). In this movie, focus 1 (circled in Fig. 4B) hardly moves over the length of the time-lapse; the MSD curve has a slope of zero. Focus 2 initially moves at greater speed (in the direction of the arrow, Fig. 4B) than the other foci in a seemingly directed manner. It then stalls before continuing motion and later settling in a fixed position; from its MSD curve (Fig. 4C) the focus is seen to undergo different motion regimes. The multiple foci labeled in a region 3 seem to wobble and by eye fall into the same category of motion. When their MSD is plotted, however, it is clear that they have different rates of diffusion.

We obtained a sufficiently large number of 'full tracks' to obtain reliable insight into how TatA complexes localize, starting with diffuse localization, followed by assembly and finally settlement. Track lengths for TatA-eGFP in the movies varied from foci linked in a few consecutive frames to tracks that could be followed for several hours (> 90 linked foci). Our observations from the live imaging experiments suggest that the categories of motion exhibited by TatA (still, traveling or wobbling) are stages in a single localization sequence.

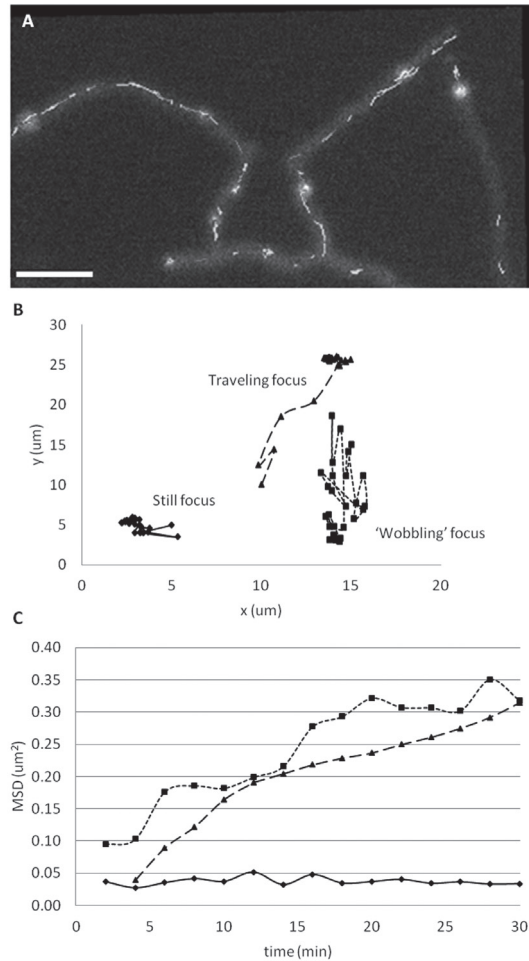


Figure 3. A trajectory and MSD analysis of dynamic TatA-eGFP localization in a *Streptomyces* hypha provides evidence for different stages of localization (frame taken from Supplemental Video 2). TatA-eGFP tracks projected onto the frame demonstrate that dynamics occur throughout entire hyphae (A). Scale bar, 5 μm . Foci could be classified into those that are still, traveling and wobbling (B); the displacement of these foci is plotted on an x-y plot, with tracks starting at (5,5), (10,10) and (15,15) respectively. The still focus stays close to its origin; the traveling focus appears to move rapidly in a directed fashion for the first part of its trajectory and then to localise; the wobbling focus has a more random trajectory. The MSD is plotted versus time for the foci shown (C). Only the first half of the curve (total time 60 min) is plotted and taken into consideration to minimise error. The still focus has a slope of zero. The traveling focus has an MSD curve with two regimes: fast, followed by slower diffusion. Linear trend lines are fitted to these two regimes. The MSD of the wobbling focus has an upward trend, but no conclusions can be drawn on the diffusion.

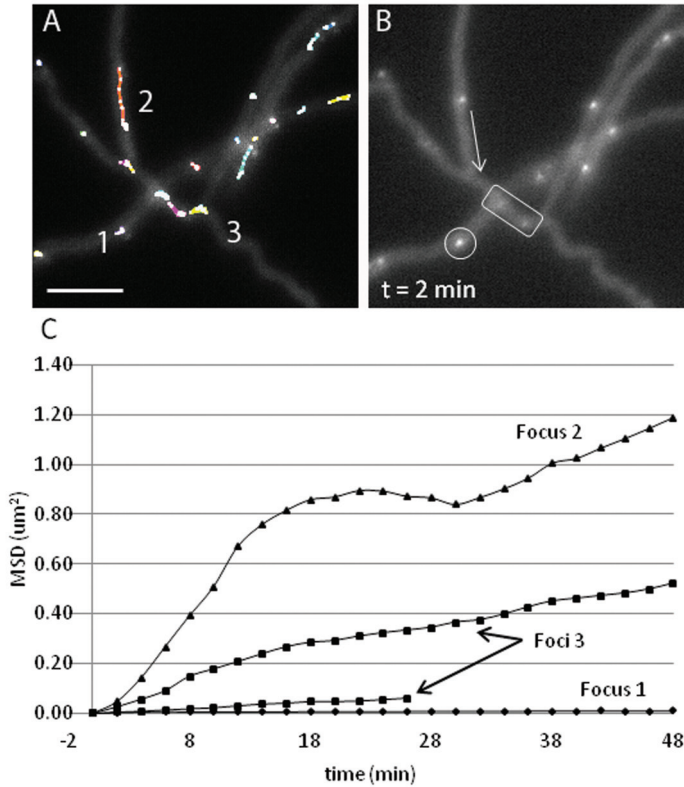


Figure 4. TatA-eGFP localizes dynamically in a *Streptomyces* hypha showing different stages of movement (frames taken from Supplemental Video 3). Detected tracks of the foci are projected onto the frame with different colours (A). Some foci are still (1), some travel linearly before stalling, continuing motion, and then become still (2) and some wobble backwards and forwards (3). For clarity, the still focus is circled, the direction of travel of focus 2 is shown with an arrow, and the portion of a hyphae where several foci (foci '3') are wobbling is denoted by a rectangle (B). Scale bar, 5 μm . The MSD is plotted versus time for the foci presented (C). Only the first half of each curve is plotted and taken into consideration to minimise error. The MSD of the still focus is zero. The traveling focus, which travels quickly, stalls, and then continues motion until localizing has an MSD with different regimes. Two foci from region 3 show different rates of diffusion.

Proteins may be observed in each of the different stages of motion in a single time lapse since dynamics within the hyphae are not synchronized. Short tracks represent foci that fade or fuse at the onset of imaging, while longer tracks undergo dynamic transition through all stages of movement. The latter start with dispersed localization, with faint foci likely

consisting of only a few TatA tetramers, followed by confined movement when tetramers oligomerize, and finally a fixed localization, at which point TatA multimers most likely colocalize with TatBC to form a functional translocation system. By taking into account only the foci that undergo all of the above stages of localization, the average time for a focus of TatA to assemble and find its proper position was estimated at between 15-30 minutes (Supplemental Figure 1).

This localization time may be indicative of the time required for an active TatABC transport complex to assemble. The current model for the Tat mechanism postulates that TatA polymerizes in response to substrate binding to the TatBC complex. The decrease in mobility during localization supports this idea and most likely represents the formation of a TatABC complex which actively transports proteins outside the bacterial cell (Leake *et al.* 2008). Our time lapse imaging in *Streptomyces* supports the notion that Tat component dynamics are very complex, with the proteins undergoing various phases of motion (and consequently rates and modes of diffusion) during localization.

Previous studies on localization of the replisome machinery in *Streptomyces* observed that most apically localized DNA replisomes were more than 1.5 μm from the tip (Ruban-Ośmiałowska *et al.* 2006), settling at a position on average 5.32 (± 2.00) μm from the tip (Wolański *et al.* 2011). Our unpublished data by high resolution electron microscopy further suggest that the very tips of hyphae are a ribosome-free area, which could also explain why the Tat complex localizes near, but not at the tip. Ribosomes are known to localize near the nucleoids, and these data would confirm a model coupling transcription with translation and subsequent secretion of certain protein products by the Tat system.

To the best of our knowledge, our analysis of TatA dynamics is the first example of a quantitative analysis of dynamic protein localization in *Streptomyces*. Study of other dynamically localizing fluorescent proteins will provide more insight into the biochemical details of protein assembly and localization. Tracking single proteins in the cell and analyzing their trajectories will significantly increase our understanding of dynamic behavior of proteins *in vivo*.

ACKNOWLEDGEMENTS

We are grateful to the organizers of the ISBI Particle Tracking Challenge 2012 for stimulating discussions. We would like to thank Tracy Palmer for providing us with the TatA-eGFP fusion constructs and for her helpful comments on the manuscript. This work was supported by a VICI grant from the Netherlands Applied Research Council (STW) to GPvW.

Supplemental Material - Supplemental Data S1

Plotting the mean-square displacement as a function of time interval can be used to characterize particle movement by determining whether diffusion is Brownian, active or constrained (Figure S1), and to calculate the diffusion coefficient. The mean square displacement is defined as:

$$MSD(t) = \langle r^2(t) \rangle = \langle |r_i(t) - r_i(0)|^2 \rangle \quad (i)$$

where $r_i(t)$ is the position of foci i at time t and the brackets represent an average on the time steps and foci. The MSD describes the average of the squared distances between a particle's start and end position for time intervals of a certain length t in a trajectory, and gives an indication of an object's pattern of motion (de Bruin, Ruthardt et al. 2007). Normal diffusion (or Brownian motion) is indicated by a linear dependence of $\langle r^2(t) \rangle$ on the time interval and can be described by:

$$MSD(t) = \langle r^2(t) \rangle = 4D\Delta t \quad (ii)$$

where D is the diffusion coefficient, and the factor 4 is specific for 2-dimensional diffusion. Confined diffusion is indicated by an asymptotic behavior at large Δt and normal diffusion at small Δt . It can be described by:

$$MSD(t) = \langle r^2(t) \rangle = \langle r_c^2(t) \rangle \left[1 - A_1 \exp\left(-\frac{4A_2 D \Delta t}{\langle r_c^2(t) \rangle}\right) \right] \quad (iii)$$

where $\langle r_c^2(t) \rangle$ is the size of the confinement, and constants A_1 and A_2 are determined by the confinement geometry. Active transport is described by a quadratic dependence of the MSD on Δt :

$$MSD(t) = \langle r^2(t) \rangle = v^2 \Delta t^2 + 4D\Delta t \quad (iv)$$

where v is the velocity of the directed motion (drift). The MSD curves for Brownian diffusion, constrained diffusion and active transport are given in Figure S1.

The accuracy of the MSD curve is affected by the time differences: the longer the MSD, the fewer time points that can be taken into account to calculate the MSD value. Analysis of MSD curves is therefore only possible for the initial portions of the curves, typically for the first third of all points, N . This results in an artificial increase in the MSD curve of a stalling focus because the average squared displacement can no longer be determined for the final

frames of the movie where the focus remains still. A certainty measure was therefore added to the plug-in to allow the user to set the minimum of number of data points needed to create the MSD curve.

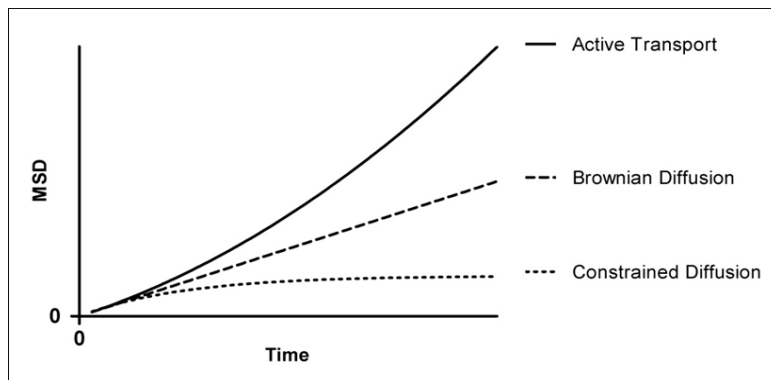


Figure S1. Mean-square displacement (MSD) curves for active transport, Brownian and constrained diffusion.

Supplemental Video, SV1

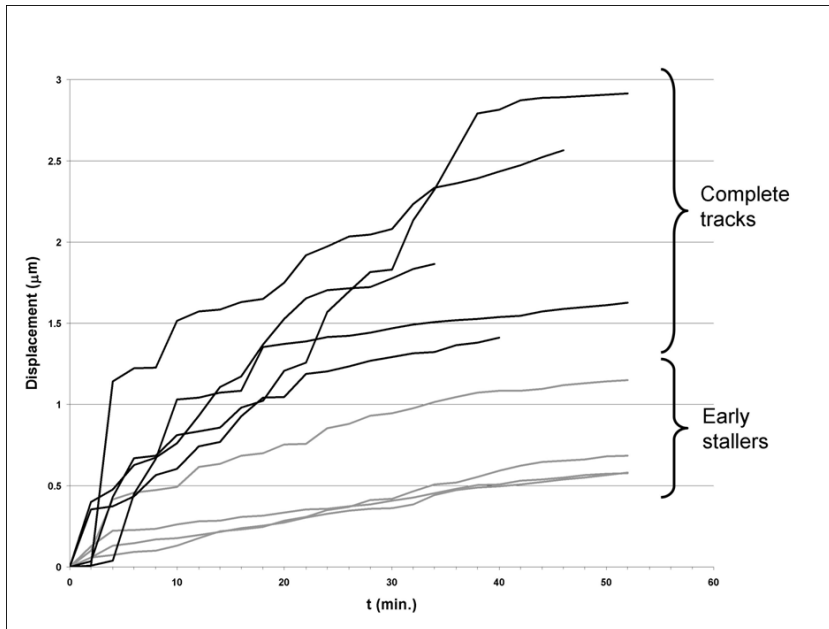
Time lapse of TatA-eGFP localizing dynamically in a *Streptomyces* hyphae. The video consists of 28 frames taken at an interval of 2 minutes between frames and plays at 6 frames per second. Total imaging time was 56 minutes. For a reference of scale, refer to Figure 1.

Supplemental Video, SV2

Time lapse of TatA-eGFP localizing dynamically in a *Streptomyces* hyphae. The video consists of 29 frames taken at an interval of 2 minutes between frames and plays at 6 frames per second. Total imaging time was 58 minutes. For a reference of scale, refer to Figure 2.

Supplemental Video, SV3

Time lapse of TatA-eGFP localizing dynamically in a *Streptomyces* hyphae. The video consists of 49 frames taken at an interval of 2 minutes between frames and plays at 6 frames per second. Total imaging time was 98 minutes. For a reference of scale, refer to Figure 3.

Supplemental Figure 1

Supplemental Figure 1. Total displacement plotted for TatA-eGFP foci with foci stalling (localizing) at different times. Visual inspection of TatA movement reveals different patterns of movement; in some cases, TatA is already assembled into a focus at the start of the movie ('early stallers'), while in others, focus assembly occurs during the time-lapse movie ('late stallers'). The assembled foci wobble, and stall at a time prior to those that assemble during the experiment, with different total displacement for each group. Averaging the curves resulted in an estimated assembly time of 15-30 minutes. The curves of complete tracks and foci already assembled at the start of imaging ('early stallers') are indicated.

Supplemental Method - Particle Tracking

A particle tracking method consists of two steps: (1) particle detection and (2) particle linking. Image analysis starts with detection of cells or fluorescent particles by segmentation. This involves partitioning of a digital image into multiple sets of pixels, and then assigning labels to these pixels such that pixels with the same label share visual characteristics. In this way, the outline of cells or fluorescent foci can be determined. Once images are segmented, a tracking algorithm is needed in order to follow a cell or focus from image to image. Here we describe our image analysis (particle detection) and tracking (particle linking) algorithm.

DETECTION

To detect particles in the images, several filtering steps are applied to enhance the contrast between natural autofluorescence and the observed particle fluorescence. The initial step for noise reduction is a Gaussian filter ($\sigma = 1$ pixel), which keeps the particles intact while the noise is diffused throughout the image. After this, two processing steps are possible, depending on the SNR in the image. For high SNRs, a top-hat filter is applied to detect and emphasize foci that are brighter than the background. The result is an image in which the background has been equalized and the foci of interest have been intensified. Based on this image, a thresholding procedure is applied, in which the cut-off intensity (above which objects are considered true particles) can be manually chosen by the user. Setting the threshold correctly is a vital part of the algorithm. In the competition, the chosen threshold values were 30 (for SNR = 7), 20 (for SNR = 4), and an automatically determined level (using the auto-thresholding function of ImageJ) with a constant added (for SNR = 1 or 2, where the constant was 10 for high-density, 12 for mid-density, and 15 for low-density images), respectively. Thresholded objects that are either too large (in this study 500 pixels or larger) or too small (less than the expected minimum size of typically 6-10 pixels depending on SNR) are filtered out. Objects located close to each other are separated using a watershed-based splitting operation, using the Euclidean distance transform. For low-SNR images, a similar approach is taken, leaving out the top-hat filter. In noisier images, this levels the background only slightly compared to the objects of interest, since these generally consist of several intensity peaks in nearby pixels. Finally, the subpixel position of each thresholded particle region is taken to be the center of mass.

LINKING

To track detected particles from frame to frame, a modified nearest-neighbor algorithm is used. Initially, the image space is divided into blocks (of tunable size, in this study 1 pixel in 2D cases, and 1 voxel in 3D cases), using a regular grid. Starting with the first frame, each particle is labeled according to the block containing its coordinates. In the next frame, the same grid is created, and the particles in that frame too are labeled according to their corresponding block. Then, each particle is linked with the particle in the previous frame that is nearest in its neighborhood, defined by the surrounding blocks (initially ± 1 block in each dimension). If multiple particles are detected, the closest one is chosen, and if none is found, the neighborhood is iteratively extended in all dimensions (to $\pm n$ blocks, $n = 1 \dots N$, with N a user-defined maximum range, typically 10). If the particles cannot be tracked within this distance, a gap-closing step is applied. This ensures that if particles disappear in a certain frame, and then reappear again, tracking continues. Gap closing is performed by running the tracking procedure on frame $t - 2$, and then continuing backwards along frames until the particle is 'found' again. Thus in a sense, particles are not tracked forwards, but backwards. The user may choose how many frames backwards to search. In this study the backwards tracking parameter was set to 3 frames. Disappearing of particles may occur due to noise or if a particle moves out of focus. Newly appearing particles are labeled as new objects and tracked thereafter in subsequent frames. If particles are tracked forward to the same particle in the next frame, the event is identified as a fusion. This is done based on particle area. It was estimated that a fusion consisting of two particles has 1.5 times the average area of a single particle, and that a fusion of three particles has 1.5 times the area of a fusion of two particles. These larger objects can be tracked back to two or three parents if these are detected in the neighborhood. Splitting particles are also detected, with both daughter particles tracking back to the same parent based on directionality. This is based on the assumption that on short time scales, tracks follow a straight path. Finally, it is possible in this method to eliminate single detections or short tracks. In the present study, single detections and tracks shorter than 3 frames were filtered out.